

# OR/18/013 The 'Rotliegend' generic model

From Earthwise

[Jump to navigation](#) [Jump to search](#)

Quinn, M, Hannis, S, Williams, J, Kirby, G, and McCormac, M. 2018. Multiscale Whole Systems Modelling and Analysis Project — A description of the selection, building and characterisation of a set of 3D generic CO<sub>2</sub> storage models. *British Geological Survey Open Report*, OR/18/013.

## Introduction

This section describes the reasoning behind the location, model build method and attribution of the generic Permian Rotliegend Leman Sandstone Formation geological model.

The model is designed to represent a depleted gas field CO<sub>2</sub> storage scenario, and is built around existing data from the Ravenspurn (North and South) gas fields, that are located approximately 50 miles east of Scarborough in the UK Southern North Sea, close to the 'feather edge' of the Rotliegend gas play (Figure 2a).

Published structural contour maps were used to build the 3D geological model, as no seismic data were available to the project. A literature review identified a suitable map over the Ravenspurn fields (Figure 4 from Ketter, 1991a<sup>[1]</sup>) that shows the faulted structure typical of the Rotliegend gas fields and fulfilled the following criteria:

- Data covering a reasonable areal extent;
- A suitable density of mapped fault structures;
- Suitable closure in both anticlinal and fault bounded structures. The fields also contain a stratigraphic closure, and therefore the field displays the three main trapping mechanisms typical of the Rotliegend.

The Ravenspurn fields are near-depleted natural gas fields located in the Southern North Sea, but for the purpose of the Whole Systems project it will be assumed that production will have ceased by the time the published Ultimately Recoverable Reserves (URR) estimate was reached. The field exhibits structural trapping in a series of NW-SE south trending fault blocks beneath thick Permian salt deposits. Stratigraphic trapping prevented hydrocarbon migration to the north. The reservoir was deposited in a desert environment and contains complex vertical and lateral facies variations, controlled in part by climatic induced variations in the water table.

The BGS structural model is based upon published structure-contour maps and the interpretation of existing well data supplemented with physical property data (described in [Data sources](#) below). Initial results of the dynamic simulation were presented at the 11th International Greenhouse Gas Control Technologies conference (Korre et al., 2013<sup>[2]</sup>).

## Geological background

### Regional geological context

The Ravenspurn gas fields are located in the UK sector of the Southern North Sea (Figure 2a),

covering part of license blocks 42/29, 42/30 and 43/26. The Leman Sandstone Formation, part of the Upper Rotliegend II (Gast et al., 2010<sup>[3]</sup>), rests unconformably over tilted and folded rocks of Carboniferous age. It in-fills topographic lows in the Base Permian Unconformity surface and thins over palaeo-highs. The regional dip of the Leman Sandstone is towards the north.

The Ravenspurn fields are some of the most northerly and deepest Rotliegend gas discoveries, lying at the northern edge of the Sole Pit Trough (Heinrich, 1991). Deposition of the Leman Sandstone occurred in a desert environment and the reservoir rocks of the Ravenspurn fields reflect a location between a playa lake, known as the Silverpit Lake to the north, and a major aeolian dune field located to the south (Figure 2.1b; Ketter, 1991a<sup>[1]</sup>; Heinrich, 1991<sup>[4]</sup>). Sabkhas were formed by windblown sand sticking to damp ground around the lake margin and in damp interdune areas. Ephemeral streams flowed roughly NNE into the Silverpit Lake (Heinrich, 1991<sup>[4]</sup>). The Silverpit Lake sediments interdigitate with reservoir sediments in the north of the field creating a stratigraphic trap which prevented hydrocarbon migration to the north. The lake eventually encroached southwards, sealing the reservoir with the overlying mudstones of the Silverpit Formation and later, the thick sequence of Zechstein Group halite which include interbedded mudstone and anhydrite.

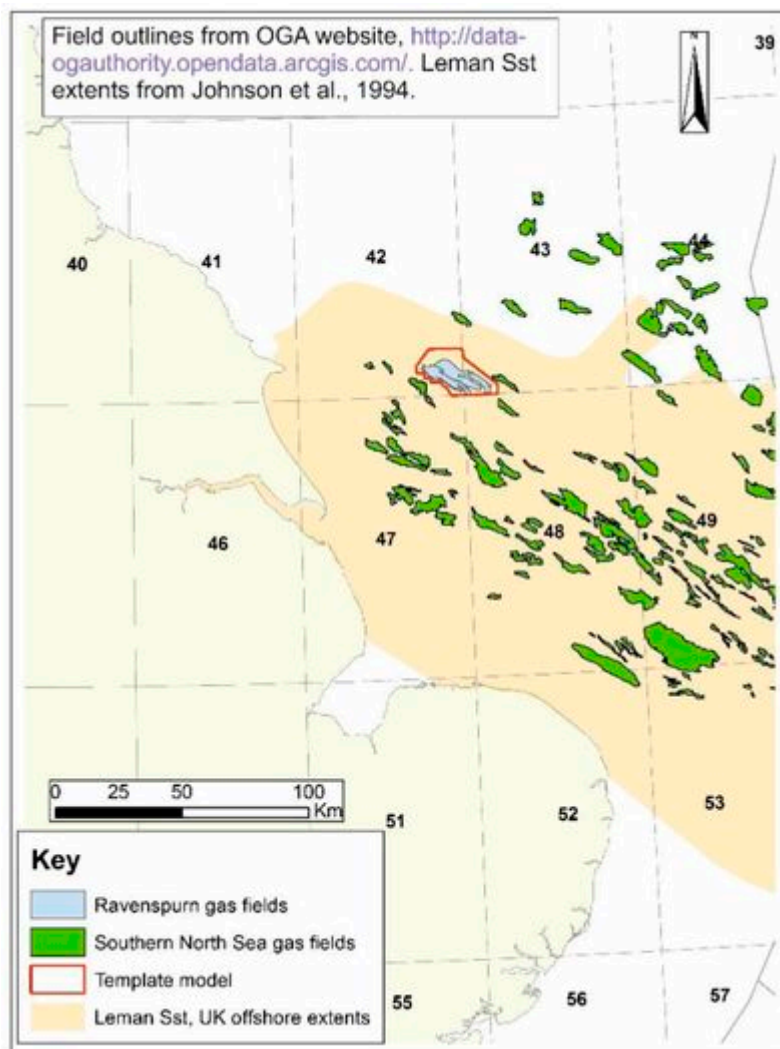


Figure 2a Location of Ravenspurn gas fields.

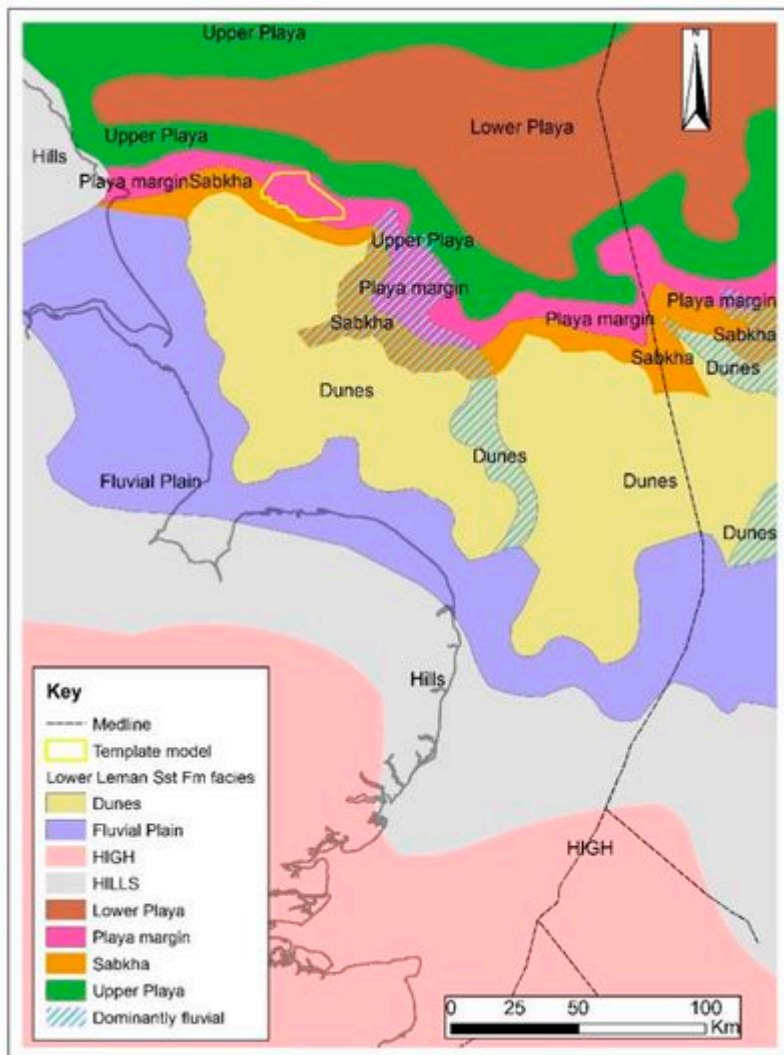


Figure 2b Palaeogeography during Upper Rotliegend (Gast et al., 2010<sup>[3]</sup>).

## Geology of the Ravenspurm gas fields

The Ravenspurm North and South gas fields cover an area of about 28 x 8 km and exhibit structural trapping in a series of normal fault blocks, predominantly orientated from northwest to southeast. The Ravenspurm North Field is divided into 'A' and 'B' structures (Figure 6), two en-echelon NW- SE-trending tilted fault blocks, located to the southwest and northeast respectively (Ketter, 1991a<sup>[1]</sup>; Turner et al., 1993<sup>[5]</sup>). An elongate periclinal structure forms an additional trap in the Ravenspurm South Field (Heinrich, 1991). The Lower Leman Sandstone Formation reservoir is juxtaposed against underlying Carboniferous strata (thought to be sealing, non- reservoir rock in this location), and against overlying Silverpit Formation and Zechstein Group rocks. The throw of some faults exceeds 200 m; however, none penetrate to the top of the Zechstein Group (Heinrich, 1991<sup>[4]</sup>).

### Facies distribution

The reservoir rocks were deposited in a desert environment marginal to a permanent lake and consist of aeolian, fluvial and sabkha facies. Non reservoir rocks include lacustrine facies. Complex vertical and lateral facies distribution was largely controlled by rising and falling water tables (Turner et al., 1993<sup>[5]</sup>; Sweet, 1999<sup>[6]</sup>).

- Aeolian sandstone is generally considered to form the best quality reservoir with porosity up to 23% and permeability up to 90 mD (Heinrich, 1991<sup>[4]</sup>). Their geometry is broadly sheet-like and

they thin towards the northwest of the field.

- Fluvial sandstones present in the Ravenspurn Fields are relatively poorer quality reservoir rocks. The poorly sorted sandstone contains more detrital clay than the aeolian deposits. They form laterally extensive ephemeral fluvial sheet flood deposits or fluvial channels with their long axis oriented in a north-north-easterly direction (Ketter, 1991a<sup>[1]</sup>).
- Sabkha deposits are highly variable reservoir rocks. Reservoir quality is good in the sandier, better sorted sabkhas but can be extremely poor in the muddier sabkhas (Sweet, 1997<sup>[2]</sup>). They can range from a few cm to several tens of cm thick, and can be laterally extensive if rising water tables allowed their preservation. Sabkha facies thicken to the northwest and dominate the upper part of reservoir.
- Lacustrine playa lake facies are non-reservoir, muddy deposits. They interdigitate with reservoir facies in the north of the field and lake encroachment to the south eventually capped the reservoir sands with the mudstones of the Silverpit Formation (Ketter, 1991a<sup>[1]</sup>).

## Controls on reservoir properties

Depositional characteristics (i.e. facies distribution) represent the primary control on reservoir porosity and permeability properties. Reservoir quality therefore deteriorates to the northwest with the pinch out of aeolian sands and interdigitation with playa lake deposits and muddy facies (Ketter, 1991a<sup>[1]</sup>).

Diagenesis is a secondary control. The main type affecting reservoir permeability is the formation of pore throat blocking 'hairy' illite, which drastically reduces permeability. This is more prevalent in the northwest of the field, further reducing reservoir quality. Early gas emplacement in the eastern part of the North field is thought to have inhibited illite diagenesis. Gas from this area was produced without reservoir stimulation, whereas elsewhere in the field, hydraulic fracturing was necessary to effectively produce gas (Turner et al., 1993<sup>[5]</sup>).

A number of high angle E-W striking fractures (attributed to Jurassic extension) are diagenetically sealed. These are noticeably confined to the aeolian facies. This reduces reservoir permeability parallel to fracture dip, but only marginally along strike. Natural fracturing is insignificant in terms of contribution towards fluid production in the Ravenspurn Fields (Ketter, 1991a<sup>[1]</sup>; Hines, 1988<sup>[8]</sup>).

## Data sources

The geological framework model built to represent the Ravenspurn Fields is based on a published structure contour map of the Top Leman Sandstone (Figure 4 of Ketter, 1991a<sup>[1]</sup>). This map was generated from the interpretation of a dense grid of both 2D and 3D seismic data across the fields, and consists of depth contours marked in feet below sea level datum along with fault polygons. The seismic data themselves were not available to this project. The internal reservoir architecture is likely to be sub-seismic in scale.

The contours and fault polygons were used along with well formation top data, to grid an accurate surface of the Top Leman Sandstone that was then used as a trend surface along with well top data to construct a surface for the base of the Leman Sandstone reservoir (Top Carboniferous/Base Permian Unconformity). Overburden horizons were also gridded using well data, and followed the geometry of the Top Leman Sandstone surface where applicable (no seismic or contour data were available for the overburden).

Digital well data were available from the Common Data Access (CDA) website (<https://www.ukoilandgasdata.com/>), which grants access to data for BGS on behalf of research

projects.

## Data import and preparation

### Seismic map

The contour map in Ketter (1991a)<sup>[1]</sup> was digitised using ArcMap 9.2, and the resulting shapefiles projected from lat/long to UTM Zone 31N (Figure 3). The shapefiles were checked, and digitising errors corrected at this stage. The data were loaded into PETREL by converting the fault and polygon shapefiles to XYZ format column delineated text files. In the absence of detailed fault geometry data the faults were projected vertically through the reservoir. As no information on fault dip was available (only the offset at the top of the reservoir was displayed on the published contour map), a Delaunay/Voronoi triangulation script was applied to the fault polygon file in order to generate fault centre-lines from which the faults could be vertically projected. This was checked and edited against the original polygons. The contour line nodes were imported to PETREL as depth attributed points while the fault centre-lines were imported as polygon linework.

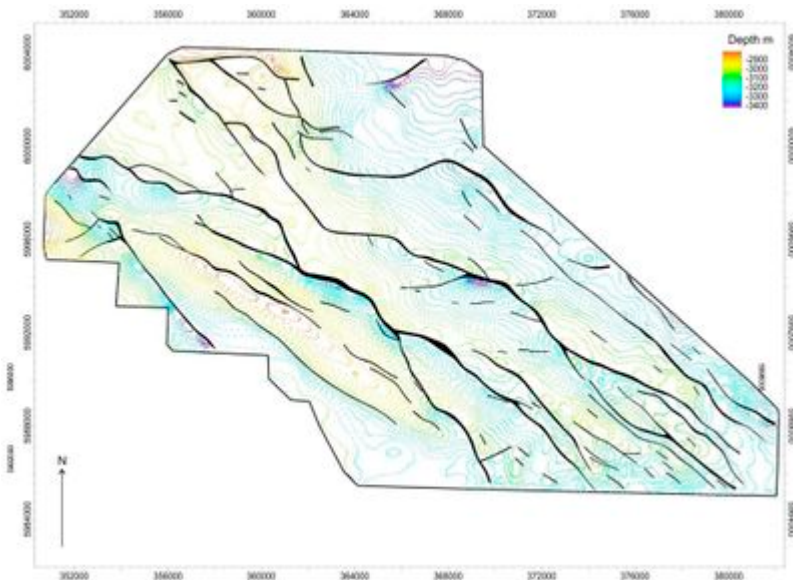


Figure 3 Structure at Top Leman Sandstone. Digitised from Ketter (1991a)<sup>[1]</sup> and imported to PETREL. Image from PETREL (fault polygons and contour points).

### Well data and well tops

A total of 80 wells were imported to PETREL for use in the 3D model (Figure 4). Vertical wells were loaded using available Kelly Bushing (KB) elevations and Total Depths (TD). Deviated well traces were loaded from digital data available from the Common Data Access (CDA) website (<https://www.ukoilandgasdata.com/>). Where digital deviation data were not available, it was obtained from tables in scanned final well reports, also taken from CDA. Wells were only included where appropriate data was available to enable the well paths to be located accurately in three dimensions. For example, well 42/30- 2 was excluded from the modelling project because the top Lower Leman Sandstone Formation observed in the well (according to the well completion report) was ~15 to 20 m lower than in surrounding wells, thus causing a dip in the top reservoir surface at the location of the well. On closer examination, the well deviation data obtained from CDA did not match the survey data listed in the well completion report. No formation depth was available in TVDSS for this well, so verification of the deviation data was not possible.

Well formation tops were obtained from company well completion logs or geological reports, and imported to PETREL as measured depths. A total of 77 well tops were loaded for the Top Lower Lemman Sandstone. No well stratigraphy data were available for the remaining three wells.

Geophysical log data for seven wells over the Lemman Sandstone interval were exported from BGS's internal database, combined with additional data from CDA, and loaded to PETREL using the built in \*.las, \*.lis or \*.dlis import filters. The well data were interpreted in the software package Interactive Petrophysics (v3.6, Senergy, 2010) to produce porosity (PHIT) and volume of shale (VWCL) curves. The resulting interpreted logs were imported into PETREL as industry-standard \*.las files. These PHIT and VWCL curves were later provided to Imperial College to be used for model attribution ([Reservoir property data](#)).

Where no digital geophysical log data were available, scanned company completion logs were cropped to the Lemman Sandstone interval, imported as portable network graphic files and attached to the appropriate wells.

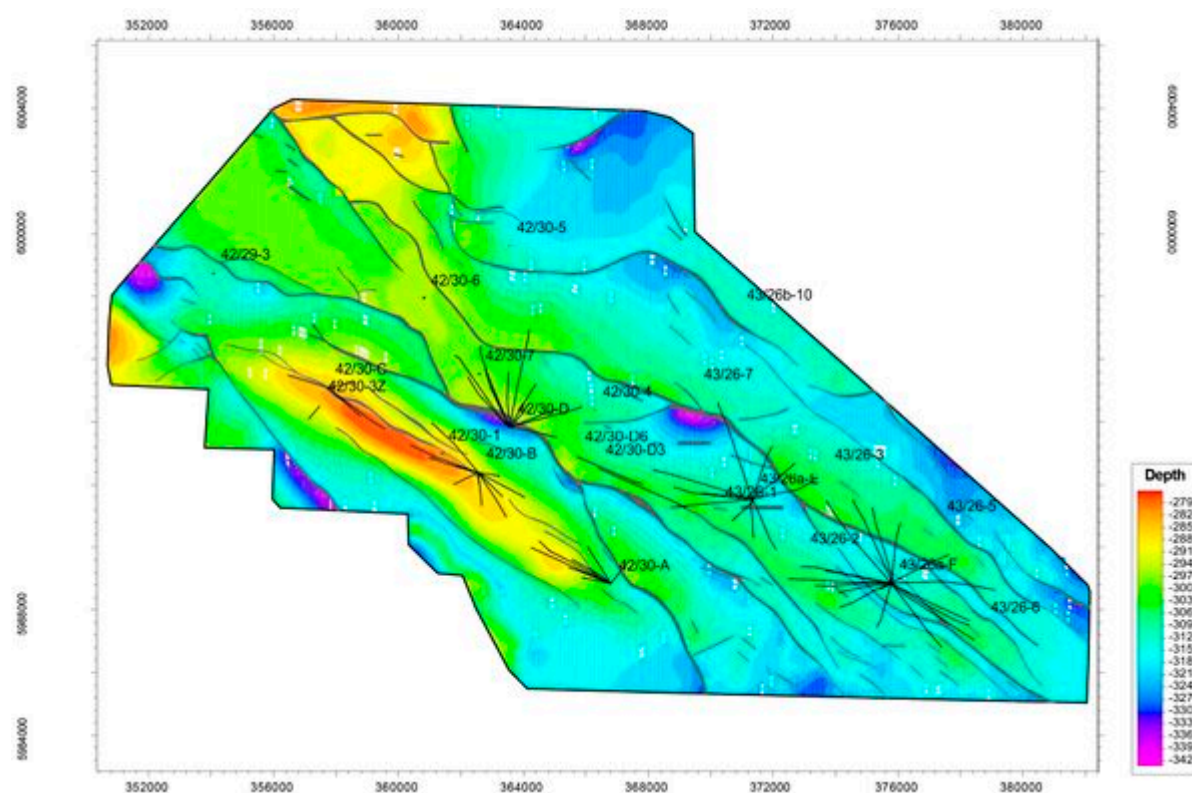


Figure 4 Location of the 80 wells in the model that penetrate the top Lower Lemman Sandstone Formation surface (coloured by Z values). Digital well data from the CDA website, <https://www.ukoilandgasdata.com/>

## Structural modelling

A top Lower Lemman Sandstone surface was constructed from the contour and fault data, which was also tied and corrected to the available well formation tops. This surface was then used as a trend surface for the other horizons that are affected by faulting. Beneath the Lemman Sandstone, the model includes a zone of Carboniferous rocks which for simplicity have been built to extend 400 m below the base of the reservoir. The real thickness of the Carboniferous is likely to be very much in excess of this, although little information is known about it specifically in this area. The 400 m Carboniferous base of the model is sufficient to ensure that the reservoir is juxtaposed against underlying strata; therefore, no gaps associated with faults exist beneath the reservoir and all reservoir-bounding faults juxtapose the Lemman Sandstone in the footwall against Carboniferous

strata where appropriate. This is important to ensure that fault juxtapositions can be represented adequately in fluid flow simulations.

Directly above the Leman Sandstone reservoir, the model includes a thickness of Silverpit mudstone, overlain by two distinct zones of the Zechstein Supergroup (comprised mainly of halite). It is known from the literature that the faults affecting the Ravenspurn fields extend to somewhere around the top of the Z2 Zechstein cycle (the top of the lower of the two Zechstein zones mentioned previously, referred to hereafter as the Lower Zechstein horizon). To represent this in the model, the faults were built to extend to the Lower Zechstein horizon. This causes a limited fault offset at the Lower Zechstein horizon, while the offset becomes absent towards the top of the model (the top of the Upper Zechstein). Formations of Triassic-Recent age above the Zechstein (Permian) were not considered for inclusion in the model, as we would not expect CO<sub>2</sub> injection to take place if it were possible for the CO<sub>2</sub> to migrate through the sealing Permian formations. The top Silverpit Formation, and top Lower and Upper Zechstein surfaces were gridded using well formation top data.

The top Upper Zechstein surface (i.e. the top of the model) was built using available well tops and control points to create a realistic representation of the Permian-Triassic boundary, which is unaffected by faulting, and therefore does not follow the faulted trend of the Leman Sandstone surface.

In summary, six main horizons separate five main geological zones in the model (Figure 5):

- Top Upper Zechstein (top of model);
- Top Lower Zechstein (Top Zechstein Cycle 2);
- Top Silverpit Formation (Top Rotliegend);
- Top Leman Sandstone Formation (Top reservoir);
- Top Carboniferous (Base Permian unconformity; base reservoir);
- Base of model (400 m from base reservoir).

The Pillar model grid was built using a preferred lateral grid size of 100 m, and was orientated along dominant fault trends (northwest-southeast).

Further sub-division within the reservoir was based upon the stratigraphic units of Turner et al., 1993<sup>[5]</sup> - their Figure 6, correlated across available geophysical log sections. The 6 stratigraphic units of Turner et al., 1993<sup>[5]</sup> are apparently persistent across the whole of the Northern field. Seven wells were available for correlation of the reservoir zonation. Relative percentages of the mean zone thicknesses in the wells were used as input to the 'Make Zones' process in PETREL, in order to model the zones conformably across the model. The nature of the layering is apparent from Figure 5.

It should be noted that the 6 modelled grid zones within the reservoir do not exactly match the correlated well tops in the 7 interpreted wells due to insufficient data coverage and varying zone thicknesses between the wells. This is not considered important here because of the generic nature of the modelling exercise. Final vertical grid cell size should be determined by layering of these reservoir zones by Imperial College based on appropriate grid resolutions for upscaling and dynamic modelling.

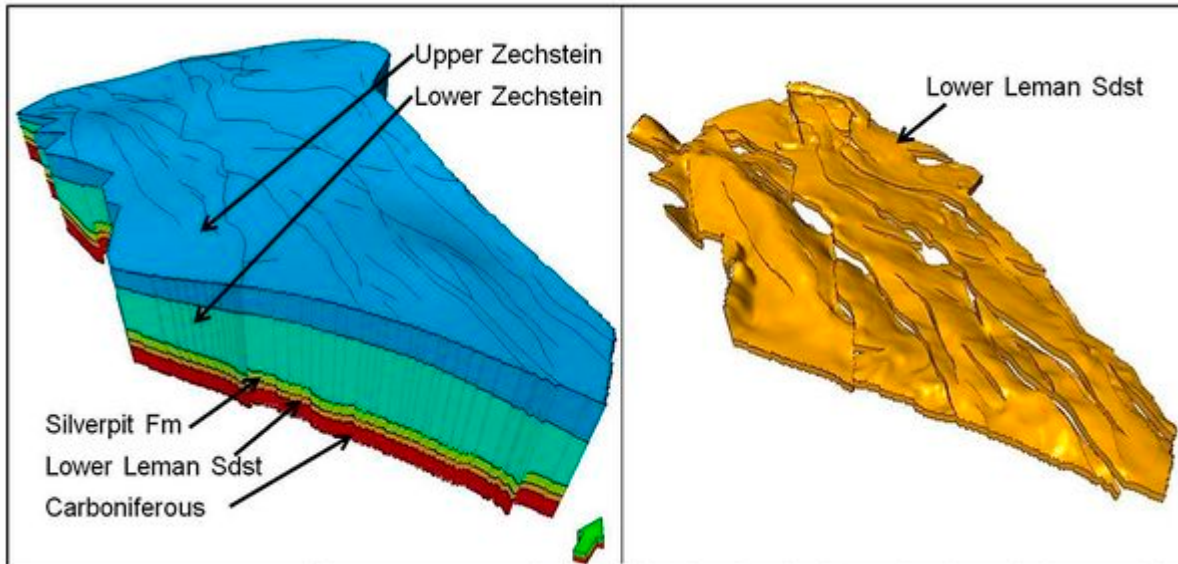


Figure 5 3D perspective view of the Ravenspurtn 3D geological model. Left: with overburden, Right: with overburden removed.

Quality control of the structural Pillar grid was achieved by visually inspecting regular cross-sections through the grid to ensure that fault throws were consistent and that intra-formational zonation did not vary significantly over short distances. Bulk volumes were also calculated to ensure that quality of the grid was good and that it did not contain any cells with negative cellular volumes. It was considered that the produced grid was sufficiently detailed for use in dynamic simulation studies, and that numerical stability should be achieved.

## Pressure and production data

A gas water contact (GWC) of 3111 m was introduced to the model based on the GWC provided by Heinrich (1991)<sup>[4]</sup> for the southern model segments and a dominant GWC of 3138 m for the northern segments (Ketter, 1991a<sup>[1]</sup>). A GWC of 3126 m in a small faulted sliver identified by Ketter (1991a)<sup>[1]</sup> was not considered significant enough to be introduced to the model, because of its small size and marginal location; it would also require further segmentation and complication of the model grid mesh. The field extent polygon was used to limit the areal distribution of the gas-bearing area. The GWC has been converted to a 'Contacts' property in the model grid. It is important to state that the GWC in the model represents the initial GWC, which may have changed significantly over the years due to production of the fields. However, if the field production was driven by gas expansion with limited or no water drive, these contact elevations may have remained consistent.

Initial pressures at Ravenspurtn North and South were 4542 and 4490 psi respectively (Heinrich, 1991<sup>[4]</sup>; Ketter 1991a<sup>[1]</sup>). No pressure data is available in the public domain for the period since production began. There are however values for the final pressure in the Leman field (also Rotliegend reservoir), which was 1/10th of the original pressure. Production here was by gas expansion with no water drive, and the recovery factor of 90% is consistent with the pressure measurements. If the drive mechanism at Ravenspurtn is also entirely by gas expansion, then the gas recovery factor of 0.62 and 0.58 for the north and south fields might suggest that the final pressures would be 0.38 and 0.42 times that of the original pressures (i.e. 1726 and 1886 psi respectively).

Production data for both fields were taken from the DECC website (now Oil and Gas Authority), <https://www.ogauthority.co.uk/data-centre/data-downloads-and-publications/production-data/>.

# Reservoir property data

Data on reservoir properties and internal reservoir architecture were provided for geostatistical analysis and model attribution. Data were derived from:

- Correlation of well tops of stratigraphic units within the Lemman Sandstone Formation across the model;
- Interpretation of the seven wells in the field that had digital geophysical log data;
- Analysis of core-derived porosity-permeability data sourced from Common Data Access (CDA);
- Geological context based on published papers and in-house background knowledge, data and expertise including regional porosity data (see area type description, [Definition of area types](#)).

The well data were interpreted in the software package Interactive Petrophysics (v3.6, Senenergy, 2010) to produce porosity (PHIT) and volume of shale (VWCL) curves. The resulting interpreted logs were imported into PETREL as industry-standard LAS files. These PHIT and VWCL curves were also provided to Imperial College separately for their analyses.

In-house expertise and data were particularly useful to extrapolate reservoir property trends over both Ravenspurn North and South fields, given the relative paucity of digital data and the complex depositional and diagenetic history of the field. This was of particular relevance in light of the stratigraphic trapping to the north-east of the field and the known property disparity between neighboring parts of the field due to diagenetic alteration inhibition as a result of structural tilting and the early gas emplacement.

The sketch map, Figure 6, summarises available property-related data and the structural parts of the Ravenspurn Field referred to in the following sections.

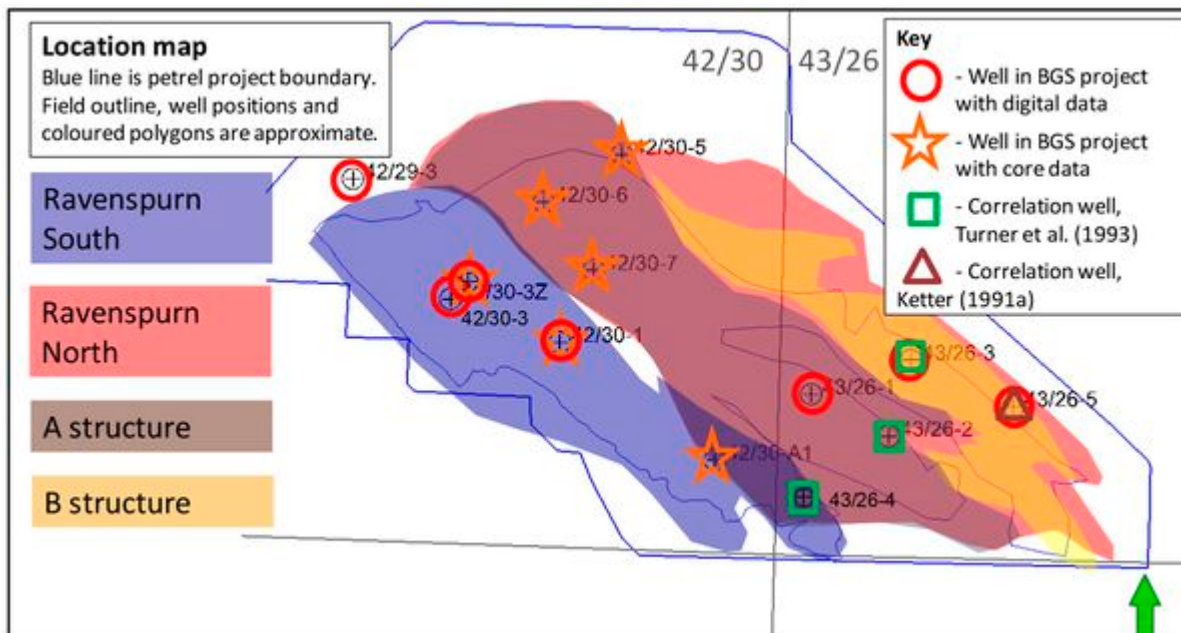


Figure 6 Map of Ravenspurn structure, with sketched shapes overlain to indicate structural regions referred to in the text and the wells with data available. Well and hydrocarbon field locations from <http://data-ogauthority.opendata.arcgis.com/>

## CORRELATION OF INTERNAL RESERVOIR ARCHITECTURE

Ketter (1991a)<sup>[1]</sup> and Turner et al. (1993)<sup>[5]</sup> subdivide the Lemman Sandstone Formation in the Ravenspurn fields into reservoir or stratigraphic zones. The stratigraphic subdivision of Turner et al.

(1993)<sup>[5]</sup> was selected to correlate across the model because the correlation was published for three wells across the field, whereas the Ketter (1991a)<sup>[1]</sup> subdivision was presented for only a single well in the North Ravenspur Field. Nevertheless, correlation over much of the Ravenspur South field was challenging due to the distances between wells with digital data.

Turner et al. (1993)<sup>[5]</sup> subdivided the Ravenspur North Field into seven lithofacies associations, representing a prevalence of either aeolian deposits (units 1-3) or those from a fluvial-playa lake depositional environment (units 4-7). The lowermost unit, unit 1, has the most variable thickness, as the deposits fill topographic lows in the underlying Carboniferous.

The raw digital logs were used to continue the Turner et al. (1993)<sup>[5]</sup> correlation across the Ravenspur fields, picking unit tops in PETREL (as well tops). Creating surfaces from these resulted in an approximately layer-cake internal reservoir architecture. These were made into Zone Logs (discrete logs describing the stratigraphy of the wells) in PETREL, to allow interpreted log curves (VWCL, PHIT) to be upscaled into the correct stratigraphic unit by Imperial College, if these logs were to be used directly to attribute the model.

## **Volume of shale and net to gross**

Net to Gross (NTG) gives an indication of the amount of 'good' reservoir within each interval of interest. A NTG value was calculated for each correlated stratigraphic unit (see [Correlation of internal reservoir architecture](#)) from Volume of Clay (VWCL) curves. These were interpreted from the digital log data for the seven wells with data available in the Ravenspur Field. The tabulated NTG values (Figure 7) were provided to Imperial College, along with the VWCL logs themselves for their own analysis.

NTG is expressed as a fraction, so a NTG value closer to 1 infers better reservoir quality.

NTG = thickness of 'good' reservoir/total thickness of interval of interest.

Whether part of the interval is considered 'good' or not is determined by applying a cut-off to a volume of clay curve (VWCL). This curve gives an indication of the 'shaleyness' of the formation where:

- 1 is considered to be 100% clay, or shale;
- 0 is considered to be 100% clean, (i.e. 0% clay or shale).

VWCL was calculated from a combination of available raw well-data curves, including gamma ray, density, neutron, caliper and density correction curves, where available. For this study a cut-off of 0.5 was used to calculate the net to gross values, i.e. where:

- If VWCL is less than 0.5, the interval is considered to be 'good' reservoir;
- If VWCL is more than 0.5 is interval is considered to contain too much clay to be a 'good' reservoir (i.e. it is considered to be non-reservoir).

Applying these parameters across the seven wells, with the available digital data, enabled calculation of NTG for the whole Leman Sandstone reservoir by stratigraphic unit. In general, the Leman Sandstone has a very high net to gross ratio (it generally contains a high proportion of clean sand). Within the Ravenspur study area the following can be said of each of the correlated units:

- Zone/units 1 & 2 are generally the poorest quality (lowest NTG) as they contain more muddy intervals;
- Zone/unit 6 is also poor quality (low NTG), except where the deposits are aeolian;

- Zone/unit 3 & 5 contain the best quality reservoir (high NTG) as they contain more aeolian facies.

Ranges of average properties for the Ravenspurh fields within each unit are shown in Figure 7.

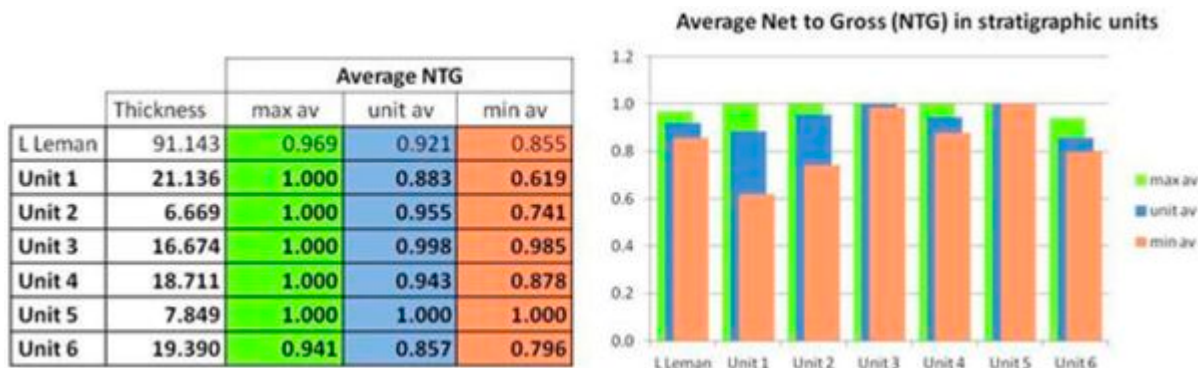


Figure 7 Average NTG values for the Lower Leman Sandstone Formation and for each individual stratigraphic unit, based on interpreted logs from 7 wells. Values in the coloured cells (left) are displayed in the corresponding coloured column on the graph (right).

In Figure 7 above, maximum, minimum and stratigraphic unit-average values of all the well data are tabulated (left) and displayed graphically (right). These data were generated using the Interactive Petrophysics ‘Multi-well cutoff and summation’ function. Note that the cut-off used for NTG calculations was a clay volume less than or equal to 0.5. Reservoir subdivisions used were those interpreted from correlation of stratigraphic units according to Turner, 1993<sup>[5]</sup> (see [Correlation of internal reservoir architecture](#)).

## Porosity distribution

Porosity data were available for the Ravenspurh Field from core data in 7 wells (Figure 6) and also from interpretation of the digital well log data (Total porosity - PHIT) for the seven wells from which the NTG was also calculated (see [Volume of shale and net to gross](#)). The PHIT averages for the formation and for each unit (see [Correlation of internal reservoir architecture](#)) were tabulated (Figure 8) along with the PHIT logs, core data and published field averages for their own analysis.

In Figure 8, the PHIT curve represents the total porosity in the formation (and as such may include unconnected porosity). This curve is interpreted from various raw and interpreted curves including density, neutron, sonic etc. The log porosity range is 2-19%.

Published information on the porosity also exists, but mainly as ranges within lithofacies, rather than by correlatable unit (which may contain a mixture of lithofacies). In the Ravenspurh South Field, Heinrich (1991)<sup>[4]</sup> reports that porosities in the aeolian sands in the upper part of the reservoir are in the 20-22% range and are lower, up to 18% in the non-aeolian deposits. Turner et al. (1993)<sup>[5]</sup> tabulated mean porosities for the North Field reproduced below (Table 3).

Table 3 Published mean porosity values (%) for the Ravenspurh North Field (Turner et al., 1993<sup>[5]</sup>).

Lithofacies	Mean porosity (%)	
	A structure	B structure
Aeolian dune/dune base	18.1	13.3
Cross-stratified fluvial	10.8	9.4
Structureless fluvial	5.9	7.5

	Thickness	Average PHIT		
		max av	unit av	min av
L Leman	91.143	0.117	0.091	0.057
Unit 1	21.136	0.135	0.078	0.028
Unit 2	6.669	0.117	0.080	0.020
Unit 3	16.674	0.170	0.125	0.066
Unit 4	18.711	0.115	0.085	0.044
Unit 5	7.849	0.196	0.118	0.036
Unit 6	19.390	0.084	0.060	0.040

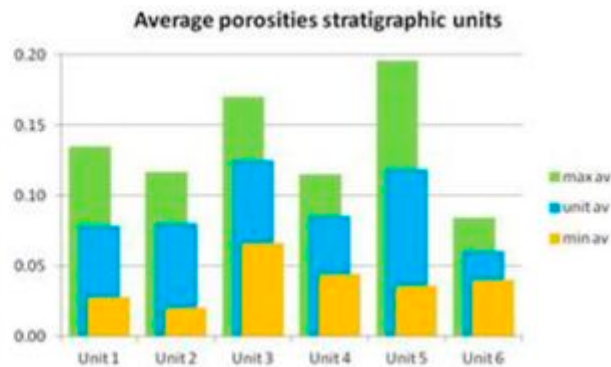


Figure 8 Average log-derived total porosity (PHIT) values for the Lower Leman Sandstone Formation and for each individual stratigraphic unit, based on interpreted logs from 7 wells. Values in the coloured cells (left) are displayed in the corresponding coloured column on the graph (right).

## Permeability ranges

Permeability data were available for the Ravenspurn fields from core data in 7 wells (Figure 6). Horizontal permeability data were available in all of the competent core samples that also had porosity data, and vertical permeability was available from a few samples. These were provided to Imperial College, along with published field averages for their own analysis.

Heinrich (1991)<sup>[4]</sup>, reported permeabilities of 10–90 mD for the aeolian, upper parts of the reservoir and low, 1 mD permeabilities for the non-aeolian parts in the Ravenspurn South field.

Turner et al. (1993)<sup>[5]</sup> reported differences in permeability between the A and B structures in the Ravenspurn North field (Figure 9). The A structure has lower permeability to the northwest, due to a reduction in aeolian facies and an increase in illite content. The B structure has better permeability as illitisation was inhibited by early gas emplacement. Anisotropic permeability is also reported, due to sealed fractures (high angle, E-W strike) which reduce the permeability parallel to the fracture dip (Turner et al., 1993<sup>[5]</sup>).

## Reservoir quality and property trends

The Ravenspurn North and South fields are known to be affected by a number of depositional and diagenetic factors that lead to a complex distribution of reservoir properties (Figure 9). Main controls include variation in facies texture (better grain sorting, roundness and packing results in better quality reservoir) and diagenesis (less diagenesis generally results in better quality reservoir).

The property trends listed below are based mainly on observations from Ketter (1991a)<sup>[1]</sup>, Turner et al. (1993)<sup>[5]</sup> and Heinrich (1991)<sup>[4]</sup>.

In a northwesterly direction there are trends in:

- Decreasing NTG;
- Decreasing porosity;
- Decreasing permeability.

This is largely due to the thinning and facies change (shaling out) of the reservoir formation in this direction, as the Leman Sandstone Formation interdigitates with the Silverpit mudstone (lacustrine deposits). Cementation and diagenetic alteration of the increased clay content to pore-throat

blocking illite has reduced the permeability resulting in the stratigraphic trap in the northwest of the field.

In a southwesterly direction, there is a trend in:

- Decreasing permeability — this is due to illitisation prior to late gas emplacement. The northern parts of the structure in the north field (B structure) were 'protected' from diagenesis by early gas emplacement, due to structural tilt of the field during the mid-late Jurassic. During production, this resulted in hydraulic fracture stimulation being required for some wells outside of the B structure (42/30-4, 42/30-6, 42/30-7, 43/26-1, 43/26-2). Hydraulic fracture stimulation was not required for wells in the B structure (43/26-3, 43/26-5, 43/26-6, 43/26-7). It is not known if stimulation in the South Ravenspur Field was required.

In the vertical direction (downwards), there are trends in:

- Decreasing porosity;
- Decreasing NTG;
- Decreasing permeability.

The increasing clay content towards the base of the formation is a result of depositional factors: The generally poorer lithofacies of the basal units have higher clay content. This increase in clay correspondingly reduces the permeability. The porosity reduction (and in part the permeability reduction also) is a result of burial compaction and cementation. Observations suggest that there is a fairly strong correlation between Lemman Sandstone Formation porosity reduction with increasing depth (Figure 10).

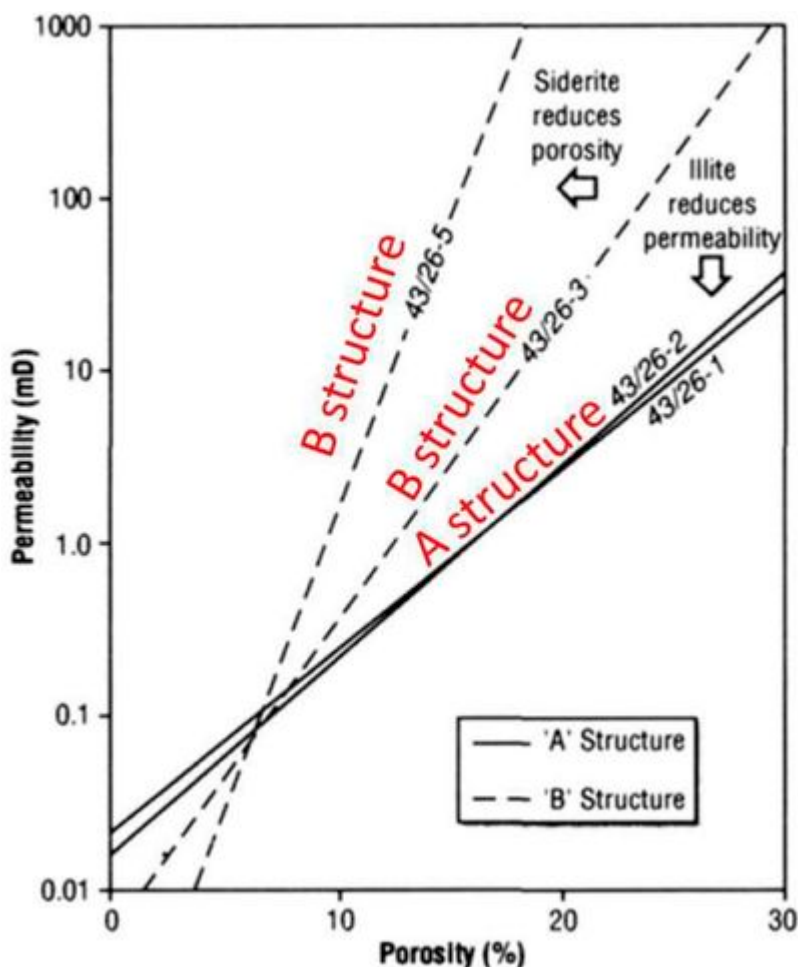


Figure 9 Porosity-permeability relationships for the

different structures in the Ravenspurn North Field, after Turner et al. (1993, his figure 11).

## Definition of area types

The variation in reservoir properties of the Rotliegend Lemman Sandstone Formation, seen in the Ravenspurn fields, will be reflected over its entire depositional extent and will affect how it behaves as a CO<sub>2</sub> store in different areas of the Southern North Sea.

It was therefore necessary to define a way in which this variation could be represented, enabling the results of the modelling of CO<sub>2</sub> injection carried out by Imperial College to be applied to other Lemman Sandstone depleted gas fields by changing the properties of the generic Rotliegend 3D geological model. A clear reduction in porosity with depth is shown by Figure 10, while the formation thickness is also directly relevant to its potential CO<sub>2</sub> storage capacity.

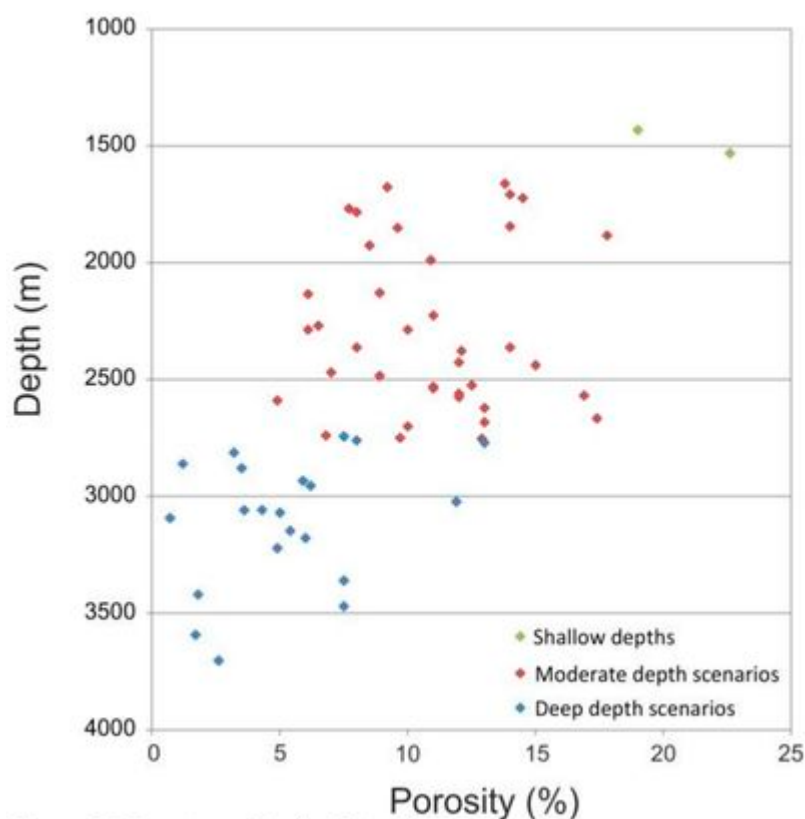


Figure 10 Porosity vs. Depth relationship.

On a regional basis, variations in both the depth to the top, and thickness of the Lemman Sandstone are regular and relatively simple but form different distribution patterns. Depths increase steadily towards the north (Figure 11), and thicknesses form a broadly elongate concentric pattern (Figure 12). By combining these parameters it was possible to define a series of 'Area Types' with storage potential (Table 4). These enable the reservoir attribution of the 3D model to be changed according to its location, defined by the Area Type. Figure 13 shows the spatial distribution of these areas. Scenarios with shallow depths (<800 m) were not considered for the purposes of this study as it is a minimum depth requirement for storage of CO<sub>2</sub> in its supercritical (dense) state (Chadwick et al., 2008<sup>[9]</sup>).

As shown in Table 4, two depth intervals and three thickness ranges were considered. The Ravenspurn fields fall into the category deep and moderate thickness. The area type categories were subsequently further sub-divided by researchers at Imperial College in order to account for

productivity variations between individual fields in the region.

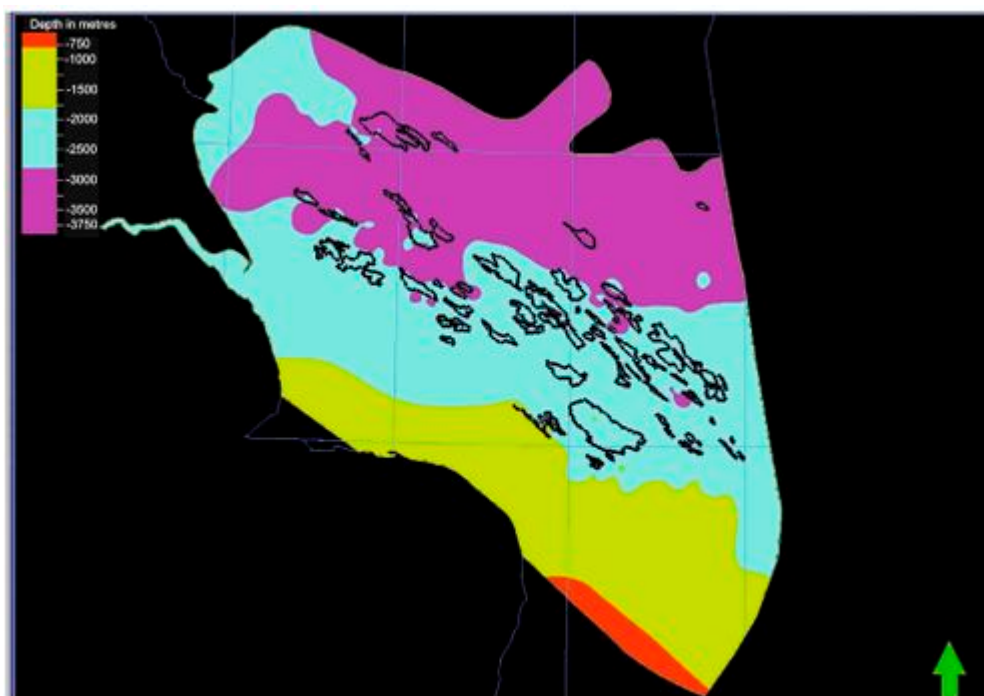


Figure 11 Depth to top Lower Leman Sandstone (m).



Figure 12 Thickness variation (m) in the Leman Sandstone reservoir.

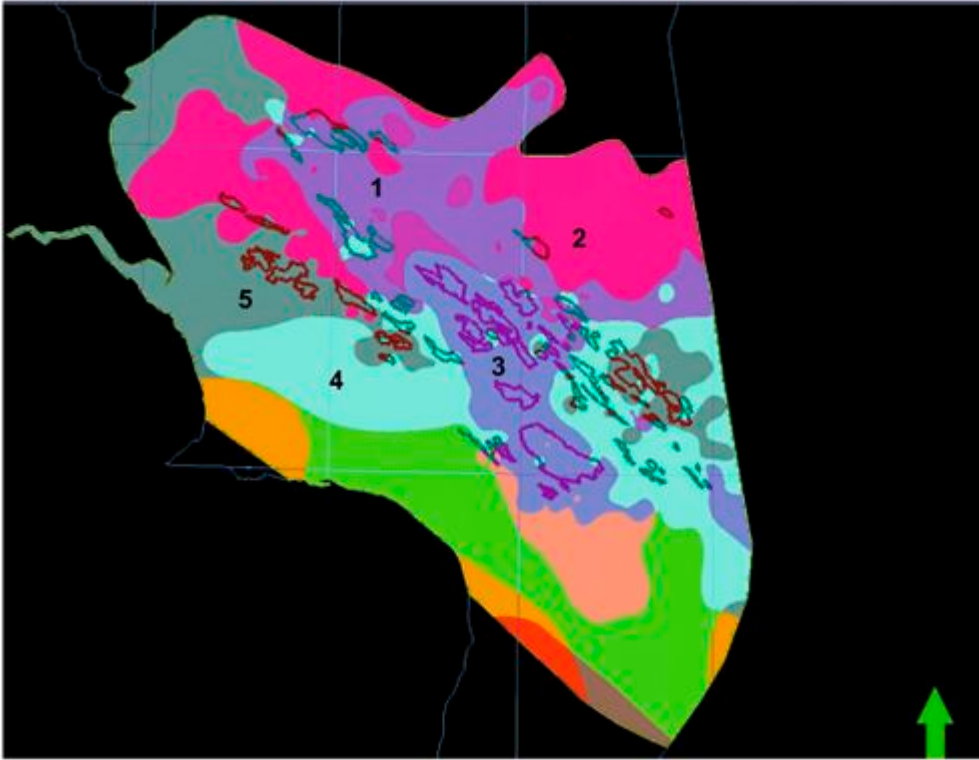


Figure 13 Rotliegend Leman Sandstone Area Types. The numbers relate to Areas described in Table 4

Table 4 Description of area type scenarios.

Area Type	Depth (m)	Thickness (m)
1	Deep: 2800–3800	Moderate: 80–180
2	Deep: 2800–3800	Thin: 0–80
3	Shallow: 1800–2800	Thick: 180–280
4	Shallow: 1800–2800	Moderate: 80–180
5	Shallow: 1800–2800	Thin: 0–80

## References

- ↑ [1.00](#) [1.01](#) [1.02](#) [1.03](#) [1.04](#) [1.05](#) [1.06](#) [1.07](#) [1.08](#) [1.09](#) [1.10](#) [1.11](#) [1.12](#) [1.13](#) [1.14](#) [1.15](#) KETTER, F J. 1991a. The Ravenspurn North Field, Blocks 42/30, 43/26a, UK North Sea. *In*: Abbotts, I L. (ed.) *United Kingdom Oil and Gas Fields, 25 Years Commemorative Volume*, Geological Society Memoir, **14**, 459–467.
- ↑ KORRE, A, DURUCAN, S, SHI, J-Q, SYED, A, GOVINDAN, R, HANNIS, S, WILLIAMS, J, KIRBY, G, and QUINN, M. 2013. Development of key performance indicators for CO<sub>2</sub> storage operability and efficiency assessment: Application to the Southern North Sea Rotliegend Group. *Energy Procedia*, **37**, pp.4894–4901.
- ↑ [3.0](#) [3.1](#) GAST, R E, DUSAR, M, BREITKREUZ, C, GAUPP, R, SCHNEIDER, J W, STEMMERIK, L, GELUK, M C, GEIBLER, M, KIERSNOWSKI, H, GLENNIE, K W, KABEL, S, and JONES, N S. 2010. Rotliegend. *In*: Doornenbal, J C, and Stevenson, A G. (eds): *Petroleum Geological Atlas of the Southern Permian Basin Area*. EAGE Publications b.v. (Houten): pp. 101–121.
- ↑ [4.0](#) [4.1](#) [4.2](#) [4.3](#) [4.4](#) [4.5](#) [4.6](#) [4.7](#) [4.8](#) HEINRICH, R D. 1991. Ravenspurn South Field, Blocks 42/29, 42/30, 43/26, UK North Sea. *In*: Abbotts, I.L. (ed.) *United Kingdom Oil and Gas Fields, 25 Years Commemorative Volume*, Geological Society Memoir, **14**, 469–475.
- ↑ [5.00](#) [5.01](#) [5.02](#) [5.03](#) [5.04](#) [5.05](#) [5.06](#) [5.07](#) [5.08](#) [5.09](#) [5.10](#) [5.11](#) [5.12](#) [5.13](#) [5.14](#) TURNER, P, JONES, M, PROSSER, D J, WILLIAMS, G D, and SEARL, A. 1993. Structural and sedimentological controls on diagenesis in the Ravenspurn North gas reservoir, UK Southern North Sea. *In*: Parker, J R. (ed.)

*Petroleum Geology of Northwest Europe: Proceedings of the Fourth Conference*, Geological Society, London, 771-785.

6. [↑](#) SWEET, M L. 1999. Interaction between aeolian, fluvial and playa environments in the Permian Upper Rotliegend Group, UK southern North Sea. *Sedimentology*. Vol. **46**, pp. 171-187.
7. [↑](#) SWEET, M L. 1997. South Ravenspurn Gas Field, offshore United Kingdom: sequence stratigraphy and heterogeneity modelling in a low permeability continental reservoir. *In*: Shanley, K W, and Perkins, B F (eds), GCS SEPM Foundation 18th Annual Research Conference: Shallow Marine and Non Marine Reservoirs, pp. 345-354, December 7-10, 1997.
8. [↑](#) HINES, M. 1988. The sedimentology of the cored lower leman sandstone in well 42/30-1, Ravenspurn South, Southern North Sea. Downloaded from CDA, report number 42/30-1rep\_GEOL\_SED\_137598997.pdf. Reports 42/30-1rep\_GEOL\_SED\_137598392.pdf and 42/30-1rep\_GEOL\_GEN\_137589871.pdf for the same well also used.
9. [↑](#) CHADWICK, R A, ARTS, R, BERNSTONE, C, MAY, F, THIBEAU, S, and ZWEIGEL, P. 2008. Best practice for the storage of CO<sub>2</sub> in saline aquifers. Keyworth, Nottingham: *British Geological Survey Occasional Publication*, **No. 14**.

Retrieved from

'[http://earthwise.bgs.ac.uk/index.php?title=OR/18/013\\_The\\_%27Rotliegend%27\\_generic\\_model&oldid=37724](http://earthwise.bgs.ac.uk/index.php?title=OR/18/013_The_%27Rotliegend%27_generic_model&oldid=37724)'

Category:

- [OR/18/013 Multiscale Whole Systems Modelling and Analysis Project - A description of the selection, building and characterisation of a set of 3D generic CO2 storage models](#)

## Navigation menu

### Personal tools

- Not logged in
- [Talk](#)
- [Contributions](#)
- [Log in](#)
- [Request account](#)

### Namespaces

- [Page](#)
- [Discussion](#)

### Variants

### Views

- [Read](#)
- [Edit](#)
- [View history](#)
- [PDF Export](#)

□

## More

## Search

## Navigation

- [Main page](#)
- [Recent changes](#)
- [Random page](#)
- [Help about MediaWiki](#)

## Tools

- [What links here](#)
- [Related changes](#)
- [Special pages](#)
- [Permanent link](#)
- [Page information](#)
- [Cite this page](#)
- [Browse properties](#)

• This page was last modified on 1 August 2018, at 08:47.

- [Privacy policy](#)
- [About Earthwise](#)
- [Disclaimers](#)

